Applied Rheology

To appear as: Appl. Rheol. 25 (2015) 53708
DOI: 10.3933/ApplRheol-25-53708

Rheological properties of southern pine oleoresins

Imane Belyamani[1], Joshua U. Otaigbe[1]*, C. Dana Nelson[2], Brian L. Strom[3], James H. Roberds[2]

[1] School of Polymers and High Performance Materials, The University of Southern Mississippi, 118 College Drive #5050, Hattiesburg, MS 39406, USA
[2] USDA Forest Service, Southern Research Station, Southern Institute of Forest Genetics, 23332 Success Road, Saucier, MS 39574, USA
[3] USDA Forest Service, Southern Research Station, 2500 Shreveport Highway, Pineville, LA 71360, USA

* Corresponding author: joshua.otaigbe@usm.edu

Received: 27.5.2015, Final version: 6.7.2015

Abstract:
Despite the economic and ecologic importance of pine oleoresins, their rheology remains little explored. In this report we describe rheological properties of oleoresins produced by mature trees of four southern pines native to North America (loblolly, slash, longleaf, shortleaf). Results indicate that these oleoresins are structured fluids that exhibit viscoelastic behavior, but differ in flow behavior. Slash pine oleoresin exhibited Newtonian flow behavior while the oleoresin from the longleaf and shortleaf pines showed pseudoplastic behavior and the loblolly pine oleoresin showed Bingham fluid behavior with a yield stress of about 1.980 Pa. Temperature-dependent viscosities for the oleoresin samples studied were well described by the Arrhenius model, yielding flow activation energies ranging from 153.5 to 219.7 kJ/mol. The viscosity of the slash pine oleoresin sample was found to be less sensitive to temperature than that of the shortleaf or longleaf pine samples. The time-temperature superposition principle was successfully applied to pine oleoresins to show behavior over the temperature range of 25 - 65°C typical for a thermorheologically simple system. Such behavior is consistent with the temperature dependent viscoelastic properties found for these complex fluids, and supports the effective use of rheological evaluations for describing physical properties of pine oleoresins.

Key words: Southern pines, oleoresins viscoelasticity, crystallization, viscosity, Bingham fluid, time-temperature superposition

1 INTRODUCTION

Oleoresins produced by pine trees are complex and dynamic mixtures of phytochemicals [1]. These compounds have long been of commercial interest, having been relied on since the earliest of times to waterproof boat hulls and improve seaworthiness and durability of accessories such as ropes [2]. Commercial uses served as the genesis and namesake of the naval stores industry which, in the southeastern region of the USA, evolved to producing spirits of turpentine and raw chemicals and remained economically important for about 150 years [3]. Pine oleoresin remains the largest stock volume of essential oils in nature and continues to be a significant source for raw materials and products ranging from turpentine to fatty acids and biofuels among other diverse uses [1, 4, 5].

In addition to its direct commercial value, pine oleoresin is of interest to forest ecologists because of its role in tree resistance to insects and diseases [6, 7]. It functions as a generalized defense against any wound agent that severs oleoresin ducts in the act of penetrating the outer bark of a pine tree. The oozing oleoresin that results from wounding provides both chemical and physical resistance properties [7 - 9]. Volatile components (mostly monoterpenes) of pine oleoresin have been extensively characterized and their role in tree resistance, as well as their use as semiochemicals by insects, is well documented [5 7, 10 11]. Nevertheless, characterization of the physical properties of pine oleoresins (such as viscosity) has been challenging, primarily because of the complex chemical nature of oleoresin and structural instabilities that often develop during handling and use. The most troublesome of these has been the rapid crystallization of the oleoresin of many species, which makes the use of established methods problematic for characterizing physical properties such as viscosity.

Viscosity is an important property of pine oleoresin because it influences volume yield per unit time and thus a tree's defensive capacity against invading organisms. Nonetheless, it has only been well-characterized for one pine species (i.e. slash pine) [12, 13], largely because of problems caused by the onset and progression of crystal formation in the other species. Unlike oleoresin obtained from the other commercial southern yellow pine species (e.g. loblolly, Pinus taeda; longleaf, P. palustris; shortleaf, P. echinata) oleoresin produced by slash pine (P. elliottii) does not rapidly crystallize under field conditions. This makes it possible to transport samples from field collection sites to the laboratory where they can be stabilized at constant temperature and subjected to tradi-

Applied Rheology

To appear as: Appl. Rheol. 25 (2015) 53708
DOI: 10.3933/ApplRheol-25-53708

tional methods of viscosity determination [13]. Limited attempts have been made by us (unpublished data by Belyamani and Otaigbe as well as Strom et al.) and others [14] to measure the viscosity of oleoresins collected from other southern pine species, but temperature variation in the field and crystallization of samples have yielded unreliable results.

To address these problems, research was initiated to make use of modern rheological methods and principles to reliably characterize and interpret the flow and deformation properties of oleoresins produced by the four major southern pine species. Thus, results reported here provide a basis for additional investigations aimed at a more complete understanding of the physical properties of southern pine oleoresins, and their biological and ecological importance.

2 EXPERIMENTAL MATERIALS AND METHODS

2.1 RESIN COLLECTION

Oleoresin samples were collected from four economically and ecologically important pine species native to southeastern United States. All trees selected for sampling were clonally propagated (grafted) individuals maintained in southeastern Mississippi by the USDA Forest Service. Oleoresin was collected from a single ramet (tree) of a single clone for each of the four species studied. These clones are identified by the following designations: loblolly pine (B-123-L), shortleaf pine (MS-40), longleaf pine (27-168), and slash pine (18-26). The sampled loblolly pine clone originated from a tree growing in southeastern Texas, whereas clones representing the other three species originated from trees growing in southern Mississippi.

Sample collections were obtained by drilling a hole (0.5 cm in diameter, ~ 2.5 cm deep) into the tree at breast height (4.5 feet above ground level), then inserting a plastic screw-cap tube (15 mL) and allowing the oleoresin to flow into the tube for 4.5 to 6.5 hours. All collections were made on September 25, 2013 between late morning and early afternoon. Flow rates ranged from 0.5 to 1.6 mL/h. After removal from the sampled tree, tubes were capped and immediately stored on ice, then transported to the laboratory where they were stored at 4°C until sample processing and testing.

2.2 RHEOLOGICAL TESTING

Rheological measurements were conducted using a dual control mode dynamic rheometer (MCR 501®) from Anton Paar USA Inc. The MCR 501® permits testing under controlled shear stress (force or torque) and controlled shear rate (speed) modes. Small amplitude oscillatory shear strain sweep, flow curve, temperature sweep and frequency sweep tests were all conducted on the samples using the MCR 501®. Tests were performed using 25 mm parallel-plate geometry. A gap of 0.8 mm was adopted for all tests except for temperature sweep and frequency sweep tests for which the gap was reduced to 0.2 mm. The rheometer was configured with the P PTD200 Peltier controlled lower plate chamber, which makes possible a very fast and reliable method to thermostat samples and has an operating range of - 40 to 200°C with an accuracy of less than 0.1°C. All measurements were performed at 25 ± 0.1°C. Prior to data collection, a pre-shear strain rate of 0.016 1/s was applied to samples for 60 seconds to remove structure present and to ensure a consistent shear history.

Temperature sweep tests were performed at temperatures ranging from 25 ± 0.1°C to 120 ± 0.1°C at a rate of 10°C/min in the linear viscoelastic region (< 1 % stain amplitude). The angular frequency was fixed at 12.5 rad/s. Data for time-temperature superposition (TTS) were obtained on samples by loading onto the rheometer and performing a series of frequency sweeps between 0.1 and 100 1/s at discrete temperatures ranging between 25 ± 0.1°C and 65 ± 0.1°C. Samples were allowed to equilibrate for 5 min at each temperature before frequency sweep measurements within the linear viscoelastic region were made. All the above rheological tests were performed in triplicate and the resulting data were found to be reproducible.

3 RESULTS AND DISCUSSION

3.1 LINEAR VISCOELASTIC PROPERTIES

The strain for linear viscoelastic (LVE) response of the four oleoresin samples was first determined by performing a strain sweep test at temperatures in the range of 25 - 120°C, with an angular frequency of 12.5 rad/s. Figure 1 shows an example of the results that were recorded. In this figure, the region where the moduli are independent of the applied strain indicates the LVE region. In order to probe LVE properties of the samples, a linear strain (γ = 0.1 % for the loblolly pine oleoresin sample and γ = 0.5 % for the other species' samples) was chosen for measurements taken at 25°C. The strain dependence of the storage modulus G' for the loblolly pine sample is anomalous compared to that observed for samples collected from the other species. Note that this behavior is reproducible and consistent with the inherent sensitivity to crystallization observed for the sample obtained from this species. It should be noted that for the temperature sweep and frequency-temperature sweep tests, a

Applied Rheology

To appear as: Appl. Rheol. 25 (2015) 53708
DOI: 10.3933/ApplRheol-25-53708

0.1 % strain was selected for the loblolly pine sample whereas a 0.5 % strain was applied for the remaining pine samples.

3.2 FLOW PROPERTIES

Flow properties of the four pine oleoresins were characterized using conventional controlled shear rate flow curves formed by plotting shear stress σ against shear strain. The resulting curves are shown in Figure 2. Clearly, this figure indicates the different flow behaviors exhibited by the pine oleoresin samples for test conditions used in this study. The slash pine sample shows a relatively linear increase in stress with increasing strain over the whole shear strain rate range investigated, indicating Newtonian flow behavior. In contrast, the longleaf and shortleaf pine samples exhibit a relatively nonlinear pseudoplastic behavior that is characterized by a linear slope in the lower and upper shear rate regions separated by lower stress change in the medium shear rate range. Unlike these samples, the loblolly pine sample shows a flat initial response that changes to one with a steeper slope as shear rate increases. Oleoresin in the loblolly pine sample thus exhibits behavior characteristic of a Bingham plastic which by definition is a material that resists flow until a critical yield stress is exceeded. Like the loblolly pine oleoresin sample, "apparent yield stress" [15] behavior was detected in the medium shear rate range for the longleaf and shortleaf pine samples. Note that the term "apparent yield stress" is used here to represent the critical stress at which there is a distinct drop in viscosity as compared to the term true yield stress that is actually exhibited by very high viscosity fluids [15]. The Herschel-Bulkley model equation (Equation 1) was fitted to the data for the loblolly, longleaf and shortleaf pine oleoresin samples displayed in Figure 2. The fit was found to be excellent and the fit parameters of this model are presented in Table 1.

$$\sigma = \sigma_o + K\dot{\gamma}^n \quad (1)$$

where σ is shear stress (Pa), σ_o is yield stress (Pa), $\dot{\gamma}$ is shear rate (1/s), K is consistency coefficient (Pas^n), and n is flow behavior index. Table 1 shows that the longleaf pine oleoresin sample has a higher yield stress than the other samples, a factor that might enhance resistance to bark beetle attack via relative resistance to flow. Compared with the yield stress of the loblolly pine sample in Table 1, the Bingham model equation (Equation 2) gave a fitted yield stress value of about 1.980 Pa for the loblolly pine sample.

$$\sigma = \sigma_o + \eta\dot{\gamma} \quad (2)$$

where η is the oleoresin viscosity (Pas). It is clearly apparent from Figure 2 that the longleaf, shortleaf and loblolly pine samples exhibit non-Newtonian shear-thinning flow behavior under the test conditions used. This shear-thinning effect thus shows that the oleoresin samples differ and this may be due to differing molecular compositions and interactions.

Figure 3 shows steady shear viscosity η for the tested pine oleoresins expressed as a function of shear rate. It is clear from this figure that the viscosity of the longleaf, shortleaf and loblolly pine oleoresin samples decreased with increasing shear rate, suggesting a pseudoplastic (non-Newtonian) behavior for these samples. The viscosity of the slash pine oleoresin sample, in contrast, is relatively independent of shear rate and more closely approximates ideal Newtonian behavior. In comparison the longleaf, loblolly and shortleaf pine oleoresin samples are strongly shear thinning (i.e. viscosity decreases with increasing shear rate), implying that shearing within these samples caused their macromolecular network structure to orient with the shear plane. In other words, the viscosity (i.e. resistance to flow) at rest is elevated, but as molecules change their flow-induced structure because of shear stress, viscosity decreases.

The longleaf and shortleaf pine oleoresin samples depict the general shape of the curve representing the variation of viscosity with shear rate. The dependence of viscosity on shear rate observed for longleaf and shortleaf pine oleoresins (Figure 3) is typical for polymeric fluids subjected to shear deformation and is characterized by two limiting viscosity values at low and high shear rates (i.e. zero-shear and infinite viscosity, respectively). In contrast, the loblolly pine oleoresin sample shows Bingham plastic flow behavior, which implies that viscosity tends towards infinity at zero shear rate. However, the viscosity versus shear rate curve for this sample levels off to a limiting constant viscosity at moderate to high shear rates. We conclude that the low shear rate data give a true representation of "at rest conditions" where loblolly pine has significant crystalline structure. Our findings are in agreement with those of Hodges et al. [9] who found that the viscosity of slash pine oleoresin is significantly greater than that of longleaf, shortleaf or loblolly pines. Moreover, Mergen et al. [16] and Runckel and Knapp [17] report that monoterpene and turpentine concentrations have a strong influence on viscosities of slash and longleaf pine oleoresins. In support of this finding, Hodges et al. [9] report a negative corre-

Applied Rheology

To appear as: Appl. Rheol. 25 (2015) 53708
DOI: 10.3933/ApplRheol-25-53708

lation between total monoterpene level and viscosity for slash, longleaf and shortleaf pines but not for loblolly pine. Hodges et al. [8, 9] also report a mean viscosity of 306 stokes and a total monoterpene content of 24 % for slash pine and a mean viscosity ranging from 18 - 60 stokes for the longleaf, shortleaf and loblolly pine oleoresins with monoterpene concentrations ranging from 28 - 30 %, indicating that other factors are involved. The density of the oleoresin systems is needed to make a more direct comparison of the above kinematic viscosity data reported in the literature with the shear viscosity data of the current study. It is worthy to note that monoterpenes are primary components of pine oleoresins (Table 2) and are known to be directly related to interactions with bark beetles [8, 10, 18]. In a study carried out by Smith [19] on ponderosa pine (Pinus ponderosa Laws), the author demonstrated that the greater the oleoresin flow and the higher the limonene content, the greater the resistance to attack by the western pine beetle (Dendroctonus brevicomis). Although limonene is the most toxic of the pine monoterpenes tested against the southern pine beetle (Dendroctonus frontalis) [20], its role in tree resistance against this beetle has not been demonstrated [8].

A complex relationship between beetles and monoterpenes is not surprising, and King and de Mayo [21] suggest that limonene is derived from α-pinene, which is an interesting conversion because α-pinene has been observed to enhance attraction of the beetles to the host pine trees, while limonene was found to be highly toxic. It is well known that a number of shear-thinning fluids are thixotropic. In the current study, the observed thixotropic behavior is ascribed to isothermal, time-dependent and reversible breakdown of some particulate structure under shear, followed by structure reformation at rest [22 24]. To characterize the ability of the tested pine oleoresin samples to recover structure that was lost during shear deformation, a thixotropic loop test was performed. Figure 4 shows the flow curves observed in the up and down ramps for the imposed shear rates. The region between the up and down shear rate ramp is typically called the hysteresis loop and is a measure of the extent of structure recovery – the larger the hysteresis loop, the less degree of recovery for a material's structure. Figure 4 shows that the slash pine oleoresin sample exhibited rapid and almost complete structure recovery as expected due to its relatively Newtonian behavior. Note that the cycle time for the complete loop is the same for all four tests in Figure 4. The flow curves for the other three pine oleoresin samples show relatively greater hysteresis loops consistent with their relatively strong shear thinning behavior. Therefore, the constant viscosities observed at the higher shear rates for the longleaf, shortleaf and loblolly pine oleoresin samples (Figure 3), indicate that steady states had been attained in their structures with no further structural breakdown being possible. This confirms our conclusion that these constant viscosities are so-called infinite shear viscosities.

3.3 EFFECT OF TIME ON VISCOELASTICITY AND STRUCTURE EVOLUTION OF PINE OLEORESIN SAMPLES

Data obtained from the small amplitude oscillatory shear (SAOS) time sweep tests performed on the four pine oleoresin samples are presented in Figure 5. Values for storage modulus *G'* and loss modulus *G"* are plotted as functions of time. In this test, a fixed SAOS strain of 0.1 % and a frequency of 12.5 rad/s were applied to samples and the viscoelastic material functions monitored over time. Prior to the SAOS time sweep test, samples were pre-sheared at 0.016 s-1 for 60 seconds to remove existing structure. The tests reveal that *G"* > *G'* for all the oleoresin samples during the first 6 minutes of testing (Figure 5). Such an observation is consistent with behavior of viscoelastic fluids exhibiting the property of dominant viscous flow as well as the shear strain amplitude sweep data presented in Figure 1. The loss moduli increased slightly over the duration of the test, but the storage moduli increased at a greater rate, indicating development of some structure within the samples. However, the rate of development of these structures depended upon the pine oleoresin sample. For example, immediately after the pre-shear, the shortleaf and longleaf oleoresin samples exhibited viscous liquid behavior (*G"* > *G'*) but after only about 10 min transitioned to elastic behavior (*G'* > *G"*). In contrast, the loblolly pine sample retained its viscoelastic liquid behavior but the growth in G' indicates development of structure after the 25 min following pre shear. Unlike the other samples studied, the slash pine sample does not show a transition to solid-like behavior (*G'* and *G"* crossover) during the tested time interval. The solid-like behavior of the shortleaf, longleaf and loblolly samples is thought to be due to formation of crystalline structures during the time sweep test. It is well documented that crystal formation, as viewed with the naked eye, increases as oleoresin samples age, and that this observation is markedly different in slash pine oleoresin as compared to the other three pine species studied. The effect of rapid crystallization of oleoresin on tree resistance to invading organisms like bark beetles is uncertain but potentially important [8, 9].

3.4 EFFECT OF TEMPERATURE ON VISCOSITY AND STRUCTURE OF FRESH OLEORESIN SAMPLES

To study temperature dependence of the viscoelastic properties of the oleoresin samples, special temperature sweep tests were performed according to standard rheometric methods. In contrast to the previous tests already described, in the current special programmed temperature sweep tests fresh samples (less than 24 hours after collection) were first heated to 120°C, to melt any macro-crystallized particles that might be present in the samples, and then subjected to a linear decrease of temperature from 120 to 25°C at a rate of 10°C/min. Subsequently,

Applied Rheology

To appear as: Appl. Rheol. 25 (2015) 53708
DOI: 10.3933/ApplRheol-25-53708

a heating step to 120°C was implemented to study ability to recover structure lost due to the temperature changes applied. The resulting temperature-dependent complex viscosity curves for the four pine oleoresin samples are shown in Figure 6. It is evident from these curves that the viscosity of the loblolly, longleaf and shortleaf pine oleoresin samples is very sensitive to temperature in the tested range (i.e. viscosity dropped markedly when temperature was increased and vice versa). In contrast, the viscosity of the slash pine sample remained constant between 120 and 70°C, thus not exhibiting temperature dependency in this range. However, below 70°C the slash pine sample followed a trend similar to that of the other oleoresin samples studied. At high temperatures (80 - 120°C) the slash pine sample exhibited a higher viscosity (2.8 Pas) than did the remaining oleoresin samples studied. Nevertheless, at a temperature of 25°C, the slash and loblolly pine samples showed the lowest complex viscosity values (16050 and 9335 Pas, respectively). The longleaf pine sample was observed to have the highest complex viscosity (793000 Pas) at this temperature, whereas the shortleaf pine oleoresin sample, presented a viscosity of 311400 Pas. Temperature effects on viscosities observed for the samples were modeled using the Arrhenius equation (Equation 3):

$$\eta^* = A \cdot exp\left(\frac{E_a}{RT}\right) \quad (3)$$

where η^* is complex viscosity (Pas) at temperature T, A is material constant (Pas), E_a is flow activation energy (J/mol) for the material, R is gas constant (8.314 J/molK), and T is absolute temperature (K). Parameters in the Arrhenius equation were obtained for each oleoresin sample by linear regression of values for the logarithm of complex viscosity versus the reciprocal of absolute temperature (ln η^* versus 1/T). Plots illustrating the fit of the observed logarithm viscosity values in the heating phase to values produced by the Arrhenius equation are shown in Figure 7. Note that only the experimental data recorded in the temperature range of 80 - 25°C produced values that compare favorably with values predicted from the fitted Arrhenius equation. Coefficients of determination R^2 of at least 0.95 indicate that the Arrhenius model provided satisfactory agreement with viscosity values observed in the temperature range 80 - 25°C. Fit parameters in the Arrhenius equation are presented in Table 3. The values of flow activation energies were found to be in the range of 153.5 to 219.7 kJ/mol. Values for this parameter reflect sensitivity of viscosity to temperature change; in general, the higher the activation energy observed then the greater the effect of temperature on viscosity. Among the studied oleoresin samples, those for shortleaf and longleaf pine had the highest values for flow activation energy, and accordingly, their viscosities possessed the strongest dependence on temperature. The loblolly oleoresin sample exhibited intermediate activation energy values; thus, its viscosity was less affected by temperature compared to samples from shortleaf and longleaf pine. Finally, viscosity for the slash pine sample was the least temperature dependent since its oleoresin had the lowest flow activation energy estimate.

The flow-induced structural transitions associated with phase change in the pine oleoresin samples are indicated by changes in the viscoelastic material functions (G' and G''). Curves for these functions are illustrated in Figure 8. The observed changes in these curves are temperature and oleoresin sample dependent and are reversible as is evident from the symmetry found for the G' and G'' curves during the cooling and heating stages. Figure 8a shows changes in G' and G'' as a function of temperature for the longleaf pine oleoresin sample. Between ~ 120 and 70°C, G'' values increase continuously while G' values remain relatively constant, signifying that oleoresin behavior in this temperature region is predominantly that observed for a typical pure viscous liquid. From ~ 70 to 40°C, values for G' increase more steeply due to the formation of a crystalline network. Between ~ 40 and 25°C, G' values are observed to be higher than those for G'', implying that the oleoresin exhibits a solid-like behavior that can be ascribed to sample crystallization. During the heating stage from 25 to 120°C, a similar trend was observed but with destruction of the solid crystals occurring at about 30°C and consequent appearance of liquid like behavior as temperature increased. The loblolly pine oleoresin sample shows G' and G'' crossover with a plausible system gelation occurring between ~ 35 and 25°C for both the cooling and heating steps (see Figure 8b). Unlike the longleaf and loblolly pine oleoresin samples, the shortleaf pine sample shows two G' and G'' crossover points (at ~ 120 and ~ 25°C) and a predominant viscous liquid flow between the two solid-liquid transition points (Figure 8c). On the other hand, the slash pine oleoresin sample showed different behavior in both the heating and cooling steps (Figure 8d); for high temperatures (~ 120 to ~ 70°C), G' values are observed to be higher than those for G'', implying that oleoresin behavior is predominantly elastic within this temperature range. At approximately 70°C the oleoresin sample transitioned into a viscoelastic liquid with $G' < G''$ until ~ 25°C where $G' = G''$, indicating a potential gelation of the system.

These results suggest that the structural transition (or phase change) of pine oleoresins is reversible and temperature-dependent, regardless of the sample considered. The development of temperature-dependent molecular rearrangements in oleoresin is believed to be responsible for the observed transition from liquid-like

Applied Rheology

To appear as: Appl. Rheol. 25 (2015) 53708
DOI: 10.3933/ApplRheol-25-53708

to solid-like behavior and vice versa. In addition, we note that the observed structural transition phenomenon is seemingly independent of the level of the volatiles component (monoterpene) in the oleoresins sampled (Table 2). The existence of liquid-solid phase transitions during the cooling stage and potential evaporation of monoterpenes at 120°C confirms the experimental finding that phase change in the pine oleoresin samples is not influenced by monoterpene components. The intrinsic macroscopic crystallization (i.e. milky crystallized particles shown in Figure 9) that was observed to occur after opening storage tubes for measurements was found to differ markedly from the flow-induced solid-liquid phase transitions we described for fresh oleoresin samples (see Figure 8). The crystallization process that results in such macro-crystallized particles has been noted in several previous studies [8, 9, 25]. Although no explanation was given for how macro-crystals are formed, this type of crystallization was suggested to be detrimental to attacking bark beetles, when coupled with high rates of oleoresin flow, because the resulting crystallized oleoresin had been observed to slow beetle movement [8]. Table 4 shows values for time to crystallization assessed as time to first visual sign of crystals in the exudate reported by Hodges et al. [9] for oleoresins produced by the four major species of pines in southern U.S. Values in this table support our observations regarding appearance of the first visual signs of crystalized particles in the samples.

It may be conjectured that formation of visual macro-crystal particles is induced by the simultaneous effects of humidity and progressive monoterpene evaporation. To test this hypothesis, macroscopically crystalized pine oleoresin samples were heated to 120°C then exposed to ambient conditions for at least 24 hours. The appearance of macro-crystallized loblolly pine oleoresin before and after undergoing the temperature sweep test is shown in Figure 10. On the left-hand side of Figure 10, macro-crystalized particles appear as 'milky white' crystals a few hours after opening the storage test tube. The process of forming such crystals was found to be irreversible. After melting all crystals in the samples (by placing them on the bottom plate of the rheometer), heating to 120°C, and subsequently cooling the samples to 25°C while storing them overnight at the same temperature, crystal reformation was not observed to take place. This observation suggests the possible influence of monoterpene evaporation on visual macro-crystallization formation since at 120°C evaporation of monoterpene would be expected to be significant: The boiling point for monoterpene is about 35°C according to Tingey et al. [11]. The right-hand side of Figure 10 shows that the loblolly pine oleoresin sample had regained its fresh appearance, however it will be shown in the next section that it did not retain all its viscoelastic properties.

3.5 EFFECT OF TEMPERATURE ON VISCOELASTIC PROPERTIES OF THE MACROSCOPICALLY CRYSTALIZED PINE OLEORESIN SAMPLES

The structural transitions associated with phase changes in the macroscopically crystallized pine oleoresin samples were studied as functions of temperature. Samples were first heated to 120°C to melt the crystals. A linear decrease of temperature from 120°C to 25°C at a rate of 10°C/min was then applied, followed by a heating step to 120°C. Curves for the resulting data are presented in Figure 11. These tests were carried out under the same rheological test conditions of strain and angular frequency applied to the fresh samples shown in Figure 8. It is evident from Figure 11 that the observed flow-induced solid-liquid phase transition behavior is temperature dependent and reversible as also found in the fresh oleoresin samples (Figure 8). Furthermore, the curves tracking the evolution of *G'* and *G"* values observed for crystalized pine oleoresin samples are similar to those observed for fresh samples. Nevertheless, small differences in values for *G'*, *G"*, and gelation temperatures were detected. For instance, the potential gelation point for the crystalized longleaf pine sample (Figure 11a) occurs at a lower temperature (25 versus 40°C for the fresh sample) and an additional *G'* and *G"* crossover point occurs at 115°C. Similarly, the crystalized oleoresin sample obtained from loblolly pine (Figure 11b) shows a *G'* and *G"* crossover at 45°C and a tendency to transition to a viscoelastic solid at lower temperatures. For the shortleaf pine samples (Figure 11c) and slash (Figure 11d), slopes for the *G'* curves in the 25 - 35°C temperature range are steeper than those observed for fresh samples, indicating an abrupt breakdown of flow induced structures. In addition, the crossover points for the *G'* and *G"* curves observed for the slash pine crystalized sample occurred at higher temperatures than were seen for the fresh oleoresin sample.

The effect of the apparent crystal growth in pine oleoresin samples on their complex viscosity was also investigated as a function of temperature (Figure 12). It is apparent that complex viscosity changes are greater than those indicated by the evolution of *G'* and *G"* values, particularly at low temperatures. From the curves shown in Figure 12 it is clear that changes in the complex viscosity of crystallized pine samples are not large at high temperatures (~ 100 - 120°C) compared to changes that occurred for fresh samples (see Figure 6). However, at low temperatures, the trend observed for those samples was reversed as macro crystals formed. For example, with a η^* value of 19500 Pas at 25°C, the longleaf pine oleoresin sample became the least viscous, even though it had the greatest complex viscosity (793000 Pas) of the freshly collected samples. Similarly, the slash pine crystalized sample showed the highest complex viscosity (798500 Pas) but was the least viscous oleoresin sample (16,050 Pa.s) prior to formation of the apparent crystals.

As was shown to be true for the fresh oleoresin samples, the effect of temperatures within the range 80

Applied Rheology

To appear as: Appl. Rheol. 25 (2015) 53708
DOI: 10.3933/ApplRheol-25-53708

- 25°C on viscosity of crystalized oleoresin samples was found to be modeled well by the Arrhenius equation (see Equation 3). Following the estimation procedure described for the fresh oleoresin samples, parameters in the Arrhenius model were obtained from viscosity data collected from crystalized samples. Coefficients of determination R^2 values greater than 0.97 indicate that this procedure returned well estimated parameter values for these samples. Parameter estimates for the Arrhenius model are presented in Table 5. Values of flow activation energy reveal that values for this parameter were influenced by the formation of the milky crystallized particles, as compared to those obtained for fresh samples. With the highest activation energy estimates (199.28 - 202.19 kJ/mol), the slash pine oleoresin crystalized sample was found to have viscosities more sensitive to temperature changes than the other samples tested. On the other hand, the longleaf pine oleoresin crystalized sample was found to have the least temperature dependent viscosities, since its flow activation energies (174.17 - 178.08 kJ/mol) were the lowest values observed. Viscosity temperature dependence for the other two pine oleoresin samples did not show substantial differences from that observed for fresh samples. The preceding described results suggest that the formation of the visual milky crystals in the pine oleoresin samples is induced by progressive monoterpene evaporation accompanied by structural rearrangements that lead to changes in the viscoelastic properties of the pine oleoresins.

3.6 TIME-TEMPERATURE SUPERPOSITION PRINCIPLE

To extend the study on the temperature effect over a wide range of time scale, time-temperature superposition (TTS) principle was studied. TTS is a concept widely used in polymer physics to combine modulus data taken as a function of frequency at various temperatures for the purpose of incorporating temperature dependence into a timescale [26, 27]. The resulting master curve covers an expanded frequency range, which can be useful for approximating the behavior of a material at frequencies or times inaccessible with rheometry. To determine whether it is appropriate to apply the TTS principle to the four pine oleoresin samples in the current study, the frequency dependence of the dynamic shear moduli (G' and G'') and the complex viscosity η^* were measured at various constant temperatures as shown in Figure 13. The resulting data were superposed using a horizontal shift factor a_T to form a single master curve.

Based on the temperature sweep data presented in Figure 8, we chose the temperature range so that samples would be stable and not undergo solid-liquid viscoelastic transitions. Therefore, a temperature range from 25 to 65°C was used for the loblolly, shortleaf and slash pine oleoresin samples whereas a temperature range of 35 to 65°C was used for the longleaf pine sample. The G', G'', and η^* values obtained for the oleoresin samples were superposed by horizontal shifts of data along the frequency axis ω according to the following equations:

$$G'(\omega a_T, T_o) = G'(\omega, T) \quad (4)$$

$$G''(\omega a_T, T_o) = G''(\omega, T) \quad (5)$$

$$\eta^*(\omega a_T, T_o) = \eta^*(\omega, T) \quad (6)$$

where T_o is the reference temperature. Figure 14 shows the resulting G', G'', and η^* master curves for pine oleoresin samples at a reference temperature of 25°C (for loblolly, shortleaf and slash pine samples) and of 35°C (for the longleaf pine sample). It is evident that the viscoelastic material functions (G', G'', and η^*) for the pine oleoresin samples at various temperatures superposed well into master curves, suggesting that the TTS principle can be reliably used to interpret rheological data for pine oleoresins. This implies that pine oleoresins behave like a thermorheologically simple system, in the tested temperature range, obeying the principle of temperature and time equivalence. The successful application of the TTS principle to the experimental data of the current study confirms minimal or no structural changes occurred in the pine samples network over the experimental temperature range of the TTS experiment. The temperature dependence of the shift factors can also be studied using the WLF (Williams-Landel-Ferry) expression (Equation 7):

$$\log a_T = \frac{c_1(T - T_o)}{c_2 + (T - T_o)} \quad (7)$$

where c_1 and c_2 are the WLF parameters. Figure 15 shows the temperature dependence of shift factors as embodied in the WLF equation for the four pine oleoresin samples at the studied temperature range. It is evident from

Applied Rheology

To appear as: Appl. Rheol. 25 (2015) 53708
DOI: 10.3933/ApplRheol-25-53708

Figure 15 that the experimental data are very well described by the WLF equation as indicated by coefficients of determination ranging between 0.999 and 1 for the pine oleoresin samples studied. Based on the obtained values of c_1 and c_2, shown in Table 6, apparent activation energy E_a can be determined according to the modified form of the WLF equation [28]:

$$E_a = \frac{2.303\, Rc_1c_2T^2}{(c_2 + T - T_o)^2} \quad (8)$$

Table 6 summarizes the obtained apparent activation energy of pine oleoresin samples, as estimated from Equation 8. It should be pointed out that the Arrhenius model previously discussed describes temperature dependence of a material's viscosity in terms of a constant activation energy (Ea), whereas the WLF model describes an apparent activation energy E_a [28]. As can be seen in Table 6, for all samples the estimated apparent activation energy values increase with increasing temperature, thus indicating temperature dependence for a_T in the experimental temperature range. The temperature dependence of shift factors at the different experimental temperatures could also reflect the effect of temperature on the viscoelastic properties of the oleoresin samples, thereby confirming their temperature sensitivity already indicated by application of the Arrhenius model. The successful application of the TTS principle and the WLF model to experimental data collected from pine oleoresins, despite the complex nature and composition (volatile and nonvolatile terpenes) of these fluids, is a novel and noteworthy finding.

4 CONCLUSION

Rheological evaluation of oleoresins collected from four different southern pine species confirmed that these compounds are structured fluids that exhibit viscoelastic behavior under small amplitude oscillatory shear deformation and flow conditions. To our knowledge, this is an original report of such behavior for pine oleoresins. The results described here suggest that species-dependent flow behaviors exist for the four pine species investigated. For example, oleoresin collected from slash pine exhibited Newtonian flow behavior whereas the longleaf and shortleaf pine oleoresin samples showed pseudoplastic behavior, but oleoresin sampled from loblolly pine behaved as Bingham fluid, requiring a yield stress of about 1.980 Pa to be exceeded before proceeding to flow. The viscosity of the studied oleoresins showed temperature dependence properties that were adequately described by the Arrhenius equation. The calculated flow activation energies of all the samples ranged from 153.5 kJ/mol to 219.7 kJ/mol; the viscosity of the fresh slash pine oleoresin sample was less sensitive to temperature changes compared to that of the fresh shortleaf and longleaf pine samples, which were the most affected by temperature changes. This trend was reversed after formation of macroscopic milky crystals in the oleoresin samples; viscosity of the slash pine oleoresin sample became the most sensitive to temperature changes (199.28-202.19 kJ/mol), whereas viscosity of the longleaf pine sample became the least temperature dependent (174.17-178.08 kJ/mol). Nevertheless, viscoelastic properties of the macro-crystallized pine oleoresin samples remained temperature-dependent and reversible. In addition, the TTS principle (or WLF equation) was successfully applied to data collected from oleoresin samples, and the results produced indicate that pine oleoresin displays behavior typical for a thermorheologically simple system over the temperature range of 25 - 65°C, despite the complex composition of these compounds.

The two types solid-liquid phase transitions observed for the four pine oleoresin species tested are compatible with different defensive mechanisms exhibited by southern pines to resist attack from its most important pest, the southern pine beetle. These include a chemical defense mechanism governed by temperature dependent physical properties of oleoresin (i.e. flow, viscosity, solid-liquid transitions) and a physical defensive mechanism, based on wound sealing, that involves formation of visual crystals apparently resulting from monoterpene evaporation. To our knowledge, the viscoelastic study described here is the first of its kind, leading us to conclude that the results described will provide a basis for a better understanding of the deformation and flow properties of pine oleoresins, and of their role in tree defense against attacks by insects and diseases.

ACKNOWLEDGEMENTS

We thank Gay Flurry, Chance Parker and Felicia Ogunjube (Southern Institute of Forest Genetics) for collection of the pine oleoresin samples and Doug Streett for encouragement of this work. This research was funded by the USDA Forest Service, Southern Research Station Research Work Units 4552 and 4160 through a Cooperative Research Agreement #13-CA-11330126-088. The research work of J.U.O's former graduate students and postdocs

Applied Rheology

To appear as: Appl. Rheol. 25 (2015) 53708
DOI: 10.3933/ApplRheol-25-53708

is gratefully acknowledged.

REFERENCES

[1] Rodrigues-Corrêa KCS, Lima JC, Fett-Neto AG: Pine oleoresin: tapping green chemicals, biofuels, food protection, and carbon sequestration from multipurpose trees, Food Energy Secur. 1 (2012) 81–93.
[2] Drew J: History, in Naval Stores: Production, Chemistry and Utilization, New York (1989).
[3] Outland RB: Tapping the Pines: The Naval Stores Industry in the American South, LSU Press (2004).
[4] McCoy M: Pining for change, Chem. Eng. News 92 (2014) 17.
[5] Derfer J, Traynor S: Chemistry of Turpentine in Naval Stores: Production, Chemistry and Utilization, New York (1989).
[6] Strom B, Goyer R, Ingram L, Boyd G, Lott L: Oleoresin characteristics of progeny of loblolly pines that escaped attack by the southern pine beetle, For. Ecol. Manag. 158 (2002) 169–178.
[7] Phillips MA, Croteau RB: Resin-based defenses in conifers, Trends Plant Sci. 4 (1999) 184–190.
[8] Hodges JD, Elam WW, Watson WF, Nebeker TE: Oleoresin characteristics and susceptibility of four southern pines to southern pine beetle (Coleoptera: Scolytidae) attacks, Can. Entomol. 111 (1979) 889–896.
[9] Hodges JD, Elam WW, Watson WF: Physical properties of the oleoresin system of the four major southern pines, Can. J. For. Res. 7 (1977) 520–525.
[10] Seybold SJ, Huber DP, Lee JC, Graves AD, Bohlmann J: Pine monoterpenes and pine bark beetles: a marriage of convenience for defense and chemical communication, Phytochem. Rev. 5 (2006) 143–178.
[11] Tingey DT, Manning M, Grothaus LC, Burns WF: Influence of light and temperature on monoterpene emission rates from slash pine, Plant Physiol. 65 (1980) 797–801.
[12] McReynolds RD: Heritability and seasonal changes in viscosity of slash pine oleoresin, USDA Forest Service Research Note SE-155 (1971).
[13] McReynolds RD, Lane JM: Adapting the bubble-time method for measuring viscosity of slash pine oleoresin, Southeastern Forest Experiment Station, US Department of Agriculture, Forest Service, 147 (1971).
[14] Nebeker TE, Hodges JD, Blanche CA, Honea CR, Tisdale RA: Variation in the constitutive defensive system of loblolly pine in relation to bark beetle attack, For. Sci. 38 (1992) 457–456.
[15] Malvern Instruments: Understanding yield stress measurements (2012), http://www.atascientific.com.au/publications/wp-content/uploads/2013/02/MRK1782-01.pdf
[16] Mergen F, Hoekstra P, Echols R: Genetic control of oleoresin yield and viscosity in slash pine, For. Sci. 1 (1955) 19–30.
[17] Runckel W, Knapp I: Viscosity of Pine Gum, Ind. Eng. Chem. 38 (1946) 555–556.
[18] Schmitt J, Nebeker T, Blanche C, Hodges J: Physical properties and monoterpene composition of xylem oleoresin along the bole of Pinus taeda in relation to southern pine beetle attack distribution, Can. J. Bot. 66 (1988) 156–160.
[19] Smith RH: Formula for describing effect of insect and host tree factors on resistance to western pine beetle attack, J. Econ. Entomol. 68 (1975) 841–844.
[20] Coyne J, Lott L: Toxicity of substances in pine oleoresin to southern pine beetles [Dendroctonus frontalis, insect pests], J. Ga. Entomol. Soc. 11 (1976) 301–305.
[21] King JF, De Mayo P: Terpenoid rearrangements, Molecular rearrangements Part 2. De Mayo (Ed.), Interscience Publisher, New York (1968).
[22] Bauer WH, Collins EA: Thixotropy and dilatancy, Rheol. Theory Appl. 4 (1967) 423–459.
[23] Roscoe R: Suspensions in flow properties of disperse systems, in Flow properties of disperse systems, North Holland Publishing Company, Amsterdam (1953).
[24] Pryce-Jones J: Studies in thixotropy, Kolloid-Z. 129 (1952) 96–122.
[25] Hanover JW: Physiology of tree resistance to insects: Annu. Rev. Entomol. 20 (1975) 75–95.
[26] Katsuta K, Kinsella J: Effects of temperature on viscoelastic properties and activation energies of whey protein gels, J. Food Sci. 55 (1990) 1296–1302.
[27] Ferry JD: Viscoelastic properties of polymers, John Wiley & Sons (1980).
[28] Dean D, Husband M, Trimmer M: Time–temperature-dependent behavior of a substituted poly(paraphenylene): Tensile, creep, and dynamic mechanical properties in the glassy state, J. Polym. Sci. Part B Polym. Phys. 36 (1998) 2971–2979.

Applied Rheology

To appear as: Appl. Rheol. 25 (2015) 53708
DOI: 10.3933/ApplRheol-25-53708

Figure Captions

Figure 1: Evolution of storage modulus G' values and loss modulus G" values as a function of strain deformations applied at 25°C to each of the four pine oleoresins tested.

Figure 2: Flow properties at 25°C of the four pine oleoresin samples tested.

Figure 3: Viscosity at 25°C for the four pine oleoresins tested expressed as a function of shear rate.

Figure 4: Thixotropic loops (upward ramp closed symbols, downward ramp open symbols) for the four pine oleoresins tested.

Figure 5: Evolution of G' and G" moduli over time for the four pine oleoresin samples tested. Tests were conducted at 25°C.

Figure 6: Complex viscosity versus temperature of the tested fresh pine oleoresin samples.

Figure 7: Logarithm of experimental complex viscosity values versus the inverse of temperature and linear regression fits calculated by Arrhenius model. Plots shown are for the heating phase of tests conducted on fresh oleoresin samples.

Figure 8: Evolution of G' values and G" values as a function of temperature: (a) the longleaf pine oleoresin sample, (b) the loblolly pine oleoresin sample, (c) the shortleaf pine oleoresin sample and (d) the slash pine oleoresin sample. The curves represent behavior for fresh samples.

Figure 9: Loblolly pine oleoresin sample: (a) fresh, (b) few hours after opening the tube for measurements, and (c) 24 hours later.

Figure 10: Macro-crystallized loblolly pine oleoresin sample: (a) before the temperature sweep test, and (b) 24 hours after the test.

Figure 11: Evolution of G' values and G" values as a function of temperature: (a) the longleaf pine oleoresin sample, (b) the loblolly pine oleoresin sample, (c) the shortleaf pine oleoresin sample and (d) the slash pine oleoresin sample. The curves represent behavior for macro-crystallized samples.

Figure 12: Complex viscosity versus temperature of the tested macro-crystalized pine oleoresin samples.

Figure 13: Dependencies of dynamic shear moduli (G' and G") on angular frequency and temperature for (a) longleaf, (b) loblolly, (c) shortleaf and (d) slash pine oleoresin samples.

Figure 14: Master curves for G', G" and η^* expressed as a function of shear frequency at a reference temperature of 25°C for (a) loblolly, (c) shortleaf, and (d) slash pine oleoresin samples and of 35°C for (b) longleaf pine oleoresin sample.

Figure 15: Temperature dependence of the TTS shift factors (symbols) fitted with the WLF equation (solid lines) for pine oleoresin samples (T_o is 35°C for the longleaf pine sample and 25°C for the remaining samples).

Table 1: Fit parameters in the Herschel–Bulkley model. Values obtained for loblolly, longleaf, and shortleaf pine oleoresin samples.

Table 2: Average monoterpene levels (mg/100 mg oleoresin) of the four pine species tested. Values were derived from at least 50 trees per species all growing in Louisiana, USA with an average age of 35 to 59 years [8].

Table 3: Fit parameters for the Arrhenius model.

Table 4: Time to initial crystallization of oleoresin from the four major southern pines; Observations were made in

Applied Rheology

To appear as: Appl. Rheol. 25 (2015) 53708
DOI: 10.3933/ApplRheol-25-53708

the field and no temperature data were provided [9].

Table 5: Fit parameters for the Arrhenius model obtained from macroscopically crystallized pine oleoresin samples.

Table 6: WLF model parameters estimated for the tested pine oleoresin samples.

Applied Rheology

To appear as: Appl. Rheol. 25 (2015) 53708
DOI: 10.3933/ApplRheol-25-53708

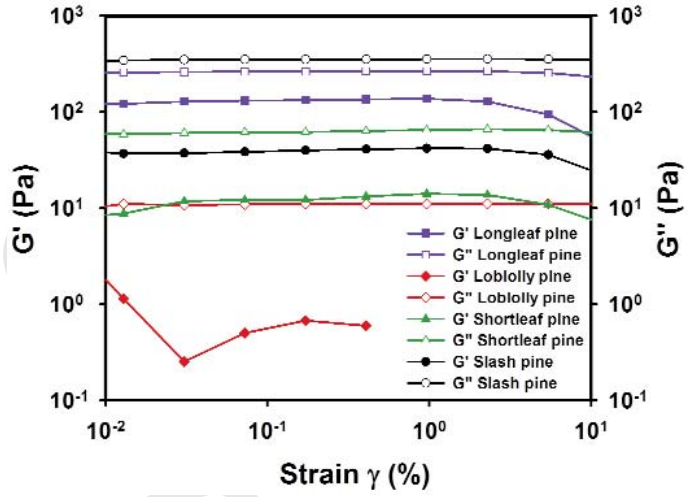

1

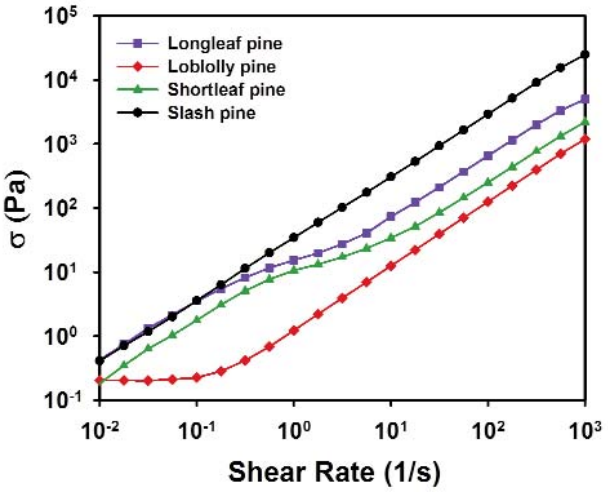

2

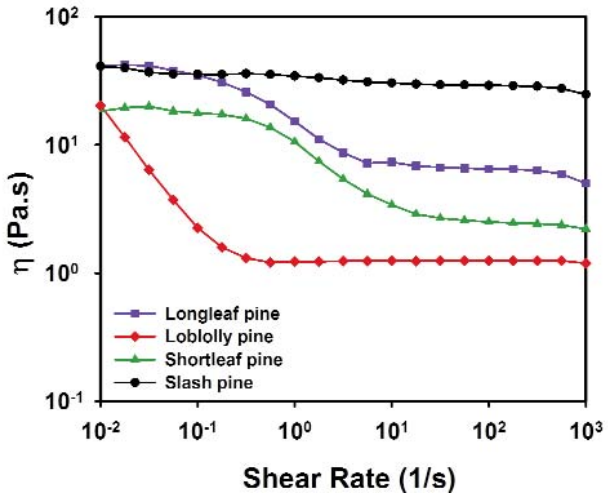

3

Applied Rheology

To appear as: Appl. Rheol. 25 (2015) 53708
DOI: 10.3933/ApplRheol-25-53708

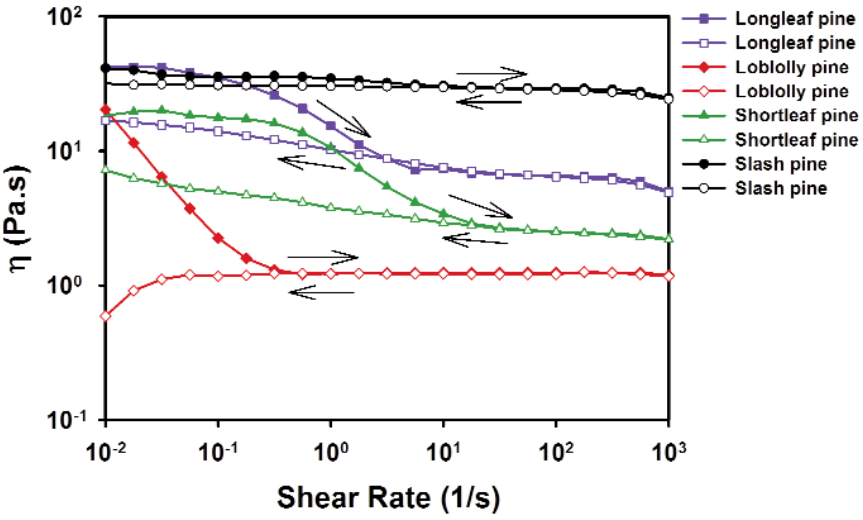

4

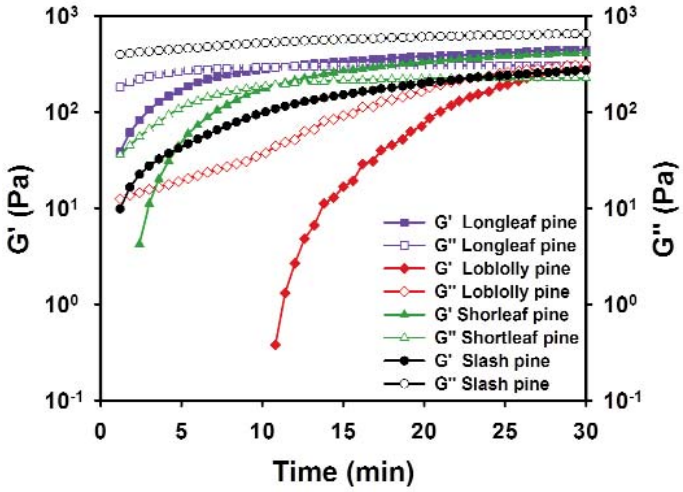

5

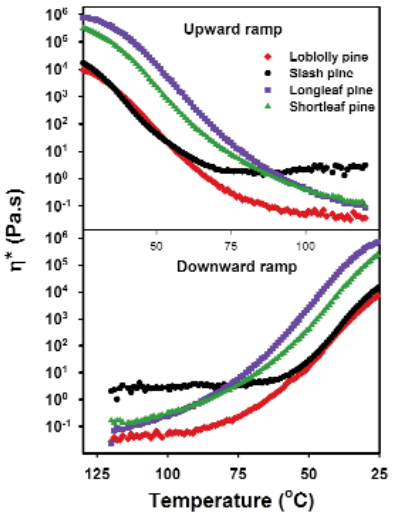

6

Applied Rheology

To appear as: Appl. Rheol. 25 (2015) 53708
DOI: 10.3933/ApplRheol-25-53708

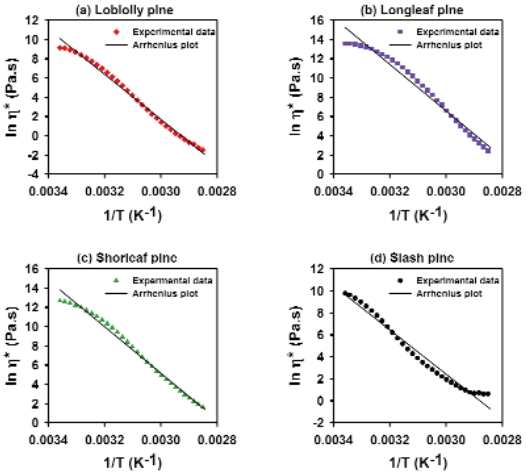

7

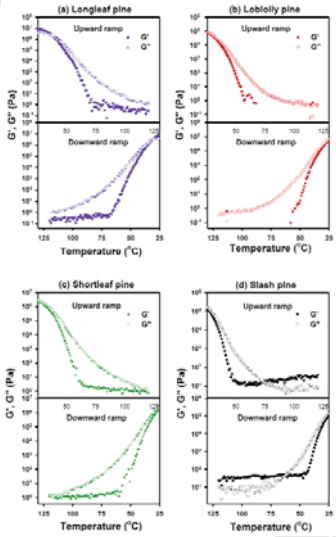

8

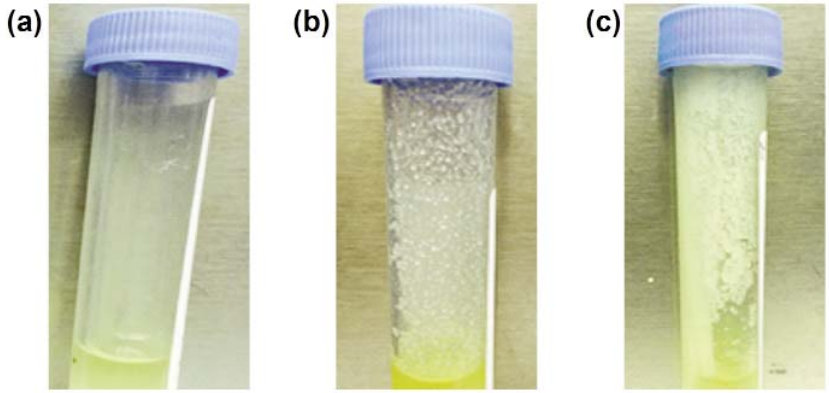

9

Applied Rheology

To appear as: Appl. Rheol. 25 (2015) 53708
DOI: 10.3933/ApplRheol-25-53708

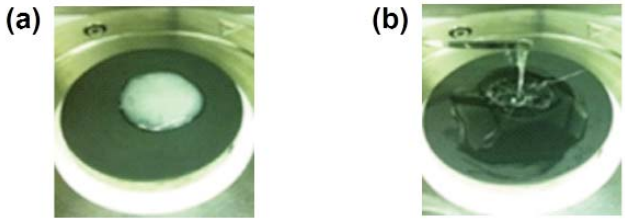

10

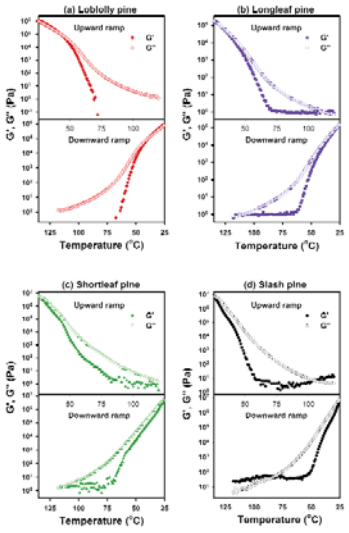

11

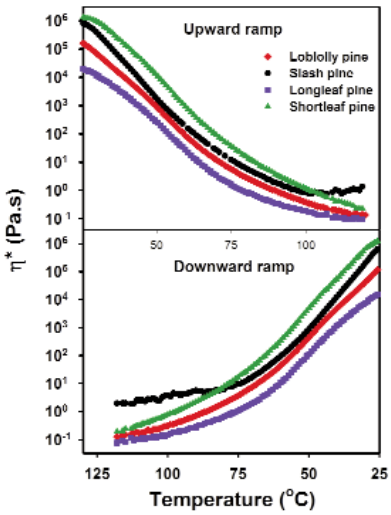

12

Applied Rheology

To appear as: Appl. Rheol. 25 (2015) 53708
DOI: 10.3933/ApplRheol-25-53708

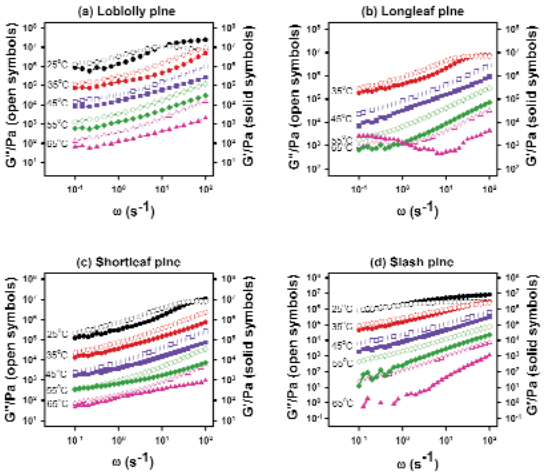

13

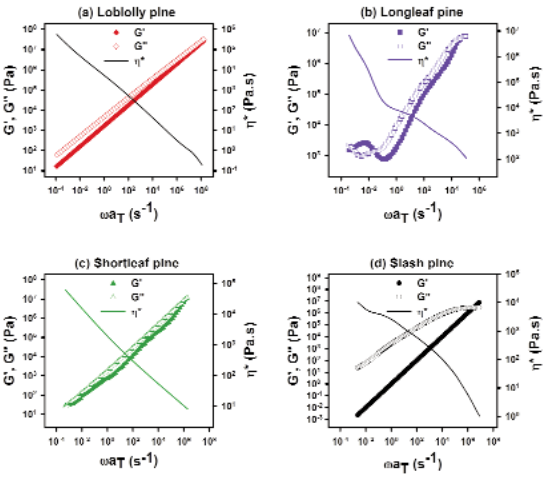

14

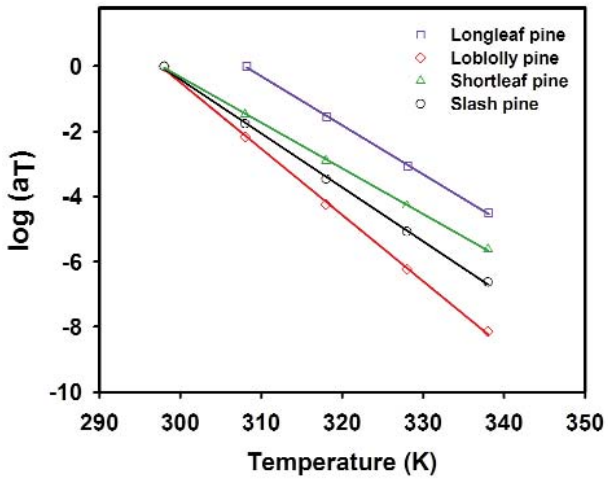

15

Applied Rheology

To appear as: Appl. Rheol. 25 (2015) 53708
DOI: 10.3933/ApplRheol-25-53708

Sample	Yield stress, σ_0 (Pa)	Consistency coefficient, K (Pa.s^n)	Flow behavior index, n	R^2
Longleaf pine	5.89	6.9	0.98	0.999
Shortleaf pine	1.83	3.84	0.88	0.990
Loblolly pine	0.2	1.24	0.99	0.999

1

Monoterpene	Loblolly pine	Shortleaf pine	Longleaf pine	Slash pine
α-Pinene	16.56	14.30	21.18	16.44
Limonene	1.68	0.93	0.49	0.25
Camphene	0.20	0.18	0.18	0.22
Myrcene	1.56	0.60	0.70	0.48
β-Pinene	8.58	12.06	5.23	4.22
β -Phellandrene	1.04	0.90	0.22	2.86

2

Species	Heating phase			Cooling phase		
	A	E_a (kJ/mol)	R^2	A	E_a (kJ/mol)	R^2
Slash pine	6.66×10^{-26}	167.4	0.974	1.1×10^{-23}	153.5	0.950
Shortleaf pine	59.7×10^{-31}	200.8	0.989	6.55×10^{-31}	203.7	0.996
Loblolly pine	1.74×10^{-30}	194.6	0.993	6.03×10^{-30}	189.3	0.995
Longleaf pine	23×10^{-32}	200.9	0.973	0.65×10^{-32}	219.7	0.994

R^2: Coefficient of determination for fit to the Arrhenius model ($\ln \eta^*$ vs. 1/T).

3

Species	Time to initial crystallization (h)
Slash pine	> 48
Shortleaf pine	2.36
Longleaf pine	0.98
Loblolly pine	0.98

4

Species	Heating phase			Cooling phase		
	A	E_a (kJ/mole)	R^2	A	E_a (kJ/mole)	R^2
Slash pine	4.29×10^{-30}	202.19	0.997	6.94×10^{-30}	199.28	0.993
Shortleaf pine	2.42×10^{-29}	197.79	0.994	1.29×10^{-28}	192.46	0.999
Loblolly pine	4.1×10^{-27}	182.49	0.973	2.33×10^{-29}	194.46	0.984
Longleaf pine	1.28×10^{-26}	174.17	0.991	1.66×10^{-27}	178.08	0.995

5

Applied Rheology

To appear as: Appl. Rheol. 25 (2015) 53708
DOI: 10.3933/ApplRheol-25-53708

Species	c_1	c_2	T (K)	E_a^* (kJ/mol)
Slash pine	187.2	450.61	298	706.39
			308	722.18
			318	737.47
			328	752.27
			338	766.60
Shortleaf pine	205.46	595.85	298	586.31
			308	605.81
			318	624.99
			328	643.84
			338	662.36
Loblolly pine	225.19	440.12	298	869.99
			308	888.52
			318	906.43
			328	923.75
			338	940.50
Longleaf pine	178.15	484.84	308	667.41
			318	682.99
			328	698.12
			338	712.82

6